

Microstructure and Electrochemical Hydrogen Storage Properties of Ball-milled $\text{Mg}_x\text{Ni}_{100-x}+5\text{wt}\%\text{TiF}_3$ ($x=50, 60, 70$) Composite

Feng HU^{1, a *}, Lei-Bo DENG^{2, b}, Qiang MA^{3, c}, Jian-Yi XU^{1, d}

¹ The School of Materials and Metallurgy, Inner Mongolia University of Science and Technology, Baotou, 014010, China

² Elected State Key Laboratory, Inner Mongolia University of Science and Technology, Baotou, 014010, China

³ School of Mathematics, Physics and Biological Engineering, Inner Mongolia University of Science and Technology, Baotou, 014010, China

^ahufengnhm_001@163.com, ^bdengleibonhm_001@163.com, ^cmaqiangnhm_001@163.com, ^dxujiany76@sina.com

*Corresponding author

Keywords: Nanostructured Intermetallics, Hydrogen Storage, Diffusion, Mechanical Alloying and Milling, Grain Boundaries, Catalysis.

Abstract. The nanocrystalline and amorphous $\text{Mg}_x\text{Ni}_{100-x}+5\text{wt}\%\text{TiF}_3$ ($x=50, 60, 70$) hydrogen storage alloys were synthesized by mechanical ball milling method. Microstructure and electrochemical performances of ball-milled alloys were characterized by X-ray diffraction (XRD), high resolution transmission electron microscopy (HRTEM), electrochemical discharge capacity and cycling stability. The results show that the ball-milled hydrogen storage alloys hold a multiphase structure consisted of two main phases Mg_2Ni and Ni as well as a small amount of third phase MgNi_2 and TiNi. The ball milling $\text{Mg}_{50}\text{Ni}_{50}+5\text{wt}\%\text{TiF}_3$ composite possesses optimal electrochemical discharge capacity, which is relevant to amorphous/nanocrystalline structure and hydride Mg_2NiH_4 phase after absorbing hydrogen. X-ray diffraction analysis indicates that ball-milled $\text{Mg}_{50}\text{Ni}_{50}+5\text{wt}\%\text{TiF}_3$ composite exhibits the best electrochemical discharge properties.

Introduction

Currently, Mg and Mg-based hydrogen storage alloy have attracted attention of researchers, being considered to be the most promising hydrogen storage materials applied in fuel cell and the negative electrode used in Ni-MH battery. However, the inherent shortcoming of Mg and Mg-based hydride, involving relatively high hydrogen desorption temperature, sluggish hydriding/dehydriding kinetics and extremely poor electrochemical cycle stability, make the practical application of the alloy become the main challenge faced by the researchers in this field. For many years, various attempts, such as mechanical alloying, surface modification and addition of catalyst, have been undertaken to improve the microstructure and hydrogen absorption/desorption properties of Mg-based hydrogen storage alloy [1-3].

Mg-Ni system Mg-based alloy holds high thermodynamic stability and poor hydriding/dehydriding kinetics, for which making the alloy engender amorphous and nanocrystalline structure is an effectual approach to improve the absorption/desorption performance by using mechanical milling technology. Liu substituted Ni with other elements in the process of preparing the glassing $\text{Mg}_{50}\text{Ni}_{50}$ alloy by mean of mechanical alloy method, and thought that the ball-milled $\text{Mg}_{50}\text{Ni}_{45}\text{M}_5$ ($M= \text{Mn, Cu and Fe}$) alloy exhibited optimum electrochemical discharge capacity and cycle stability [4]. Shao et al fabricated a series of milling Mg-Ni system alloy and investigated the effect of microstructure on hydrogen storage properties, and concluded that the $\text{Mg}_{50}\text{Ni}_{50}$ with BBC nanostructure showed more opportune absorbing/desorbing and kinetics performance, and the adding transition metal and its compound also improved the hydrogen storage properties [5]. Feng et al mechanically milled the Mg-Ni alloy with CoB for 15 h to display excellent electrochemical and kinetic characterization [6]. The

addition of Pd nanoparticle in the process of fabricating MgNi alloy through applying ball-milled technology remarkably ameliorated the absorbing/desorbing hydrogen capacity and kinetics performance [7]. Gasiorowski synthesized $Mg_{2-x}M_xNi$ ($M=Mn, Al$) alloy by MA, the electrochemical and kinetic property of it has been improved markedly [8]. The formation of MgF_2 in the process of ball milling MgH_2 using transition metal fluoride can meliorate the hydrogen releasing capacity effectually [9,10]. Jin et al [11] systematically investigated the catalysis effect of transition metal fluoride (for instance: FeF_2 , NiF_2 , TiF_3 , NbF_5 and so on) on MgH_2 , thinking that metal fluoride was an ideal catalysator in meliorating its reversible absorb and desorb hydrogen.

The objective of this work is to produce the Mg-Ni-based $Mg_xNi_{100-x}+5wt.\%TiF_3$ ($x=50, 60, 70$) nanocrystalline/amorphous alloys with mechanical ball milling and to examine the influences of the catalyst TiF_3 and Mg content on the microstructure and electrochemical hydrogen storage properties of nanocrystalline/amorphous $Mg_xNi_{100-x}+5wt.\%TiF_3$ ($x=50, 60, 70$) alloys.

Experimental

The experimental master alloys with composition of Mg_xNi_{100-x} ($x=50, 60, 70$) were prepared by using a vacuum induction furnace. In the process of smelting alloys, a helium atmosphere at a pressure of 0.04 MPa was used to prevent Mg from volatilizing in order to ensure the compose accuracy. A part of as-cast alloy ingot were pulverized into fine powder of about 200 mesh by mechanical method, then the TiF_3 was added into the alloy powder in a weight ratio of 1:0.05. The experimental composite alloy materials were synthesized by ball milling the mixture using QSM-3SP2 type planetary mill. The milling parameters, including rotation rate of 350r/min and ball to powder of 40:1 as well as duration of 60 h were automatic controlled by procedure. In the interest of preventing the rising of temperature in the milling process from changing the microstructure of samples, the ball crusher run for 3h after resting for 1 h.

The phase structures of ball-milled alloy samples were determined by X-ray diffraction (XRD) (D/max/2400). The diffraction, with the experimental parameters of 160 mA, 40 kV and 10 ($^\circ$)/min, respectively was performed with Cu $K_{\alpha 1}$ radiation filtered by graphite. The morphologies of experimental alloy were characterized by scanning electron microscope (SEM) (Philips QUANTA 400). The micrographs and crystalline state of milling alloy were observed by high resolution transmission electron microscope (HRTEM) and determined by electron diffraction (ED), respectively.

Mixing the ball-milled alloy powder with carbonyl nickel powder with a mass ratio of 1:4, the mixture was cold pressed at a pressure of 25 MPa into round electrode pellet of 15 mm in diameter and 1 g in total mass. The electrochemical measurement was performed at 30 $^\circ$ C with a tri-electrode open cell system consisting of a working electrode (hydrogen storage alloy) and a sintered $Ni(OH)_2/NiOOH$ countering electrode as well as Hg/HgO reference electrode, all electrodes were immersed in 6 mol/L KOH alkaline solution. In every cycle, the alloy electrode was first charged at a constant current density of 40 mA/g, after resting for 10 min, it was discharged at the same current density to a cut-off voltage of -0.5 V.

Results and Discussion

Microstructure Characteristics

The phase component and structure characteristics of ball-milled $Mg_xNi_{100-x}+5wt.\%TiF_3$ ($x=50, 60, 70$) composite hydrogen storage alloys are subjected to XRD analysis, just as demonstrated in Fig.1. It can be seen that the milling alloys hold multiphase structure consisting of major phases Mg_2Ni and Ni as well as secondary phases $MgNi_2$ and $TiNi$. Besides, the amount of amorphous and nanocrystalline Mg_2Ni phase increases with the rising of x content. The above-mentioned analyzing suggest that the increasing Mg content and addition of TiF_3 are helpful for forming multiphase structure as well as enhancing the glass formation ability, which can effectively

improve the absorption/desorption properties and the electrochemical cycling stability of experimental alloy sample.

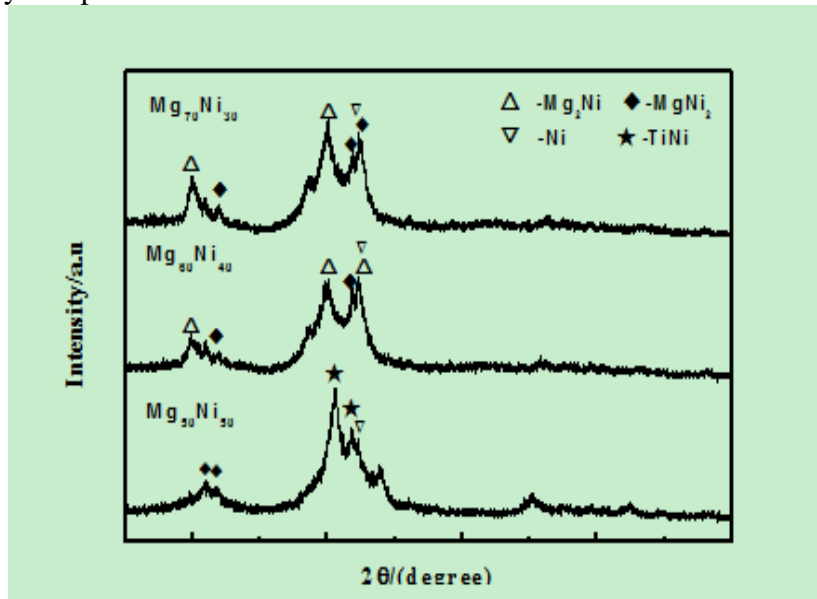


Fig. 1 XRD patterns of ball-milled $Mg_xNi_{100-x}+5$ wt.% TiF_3 ($x=50, 60, 70$) composite hydrogen storage alloy

The XRD observation is also evidenced by HRTEM, as presented in Fig.2, from which it can be found that the milled $Mg_{50}Ni_{50}+5$ wt.% TiF_3 alloy exhibits typical nanocrystalline structure and its ED diffraction rings appear sharp multi-haloes, corresponding to a crystal structure. With the rising of Mg content, the morphologies of milling alloys exhibit a feature of nanocrystalline embedded in amorphous, and their ED patterns consist of broad and dull-haloes, affirming the existence of the amorphous structure. Furthermore, the glassing degree of ball-milled experimental alloys is enhanced with the rising of the amount of Mg inside experimental alloys. Besides, through analyzing the interplanar crystal spacing of different areas in HRTEM micrograph finds that the milling $Mg_xNi_{100-x}+5$ wt.% TiF_3 ($x=50, 60, 70$) alloys bold multiphase structure, including Mg_2Ni phase, Mg phase, $MgNi_2$ phase and TiNi phase, which agree well with the XRD observations in Fig. 1.

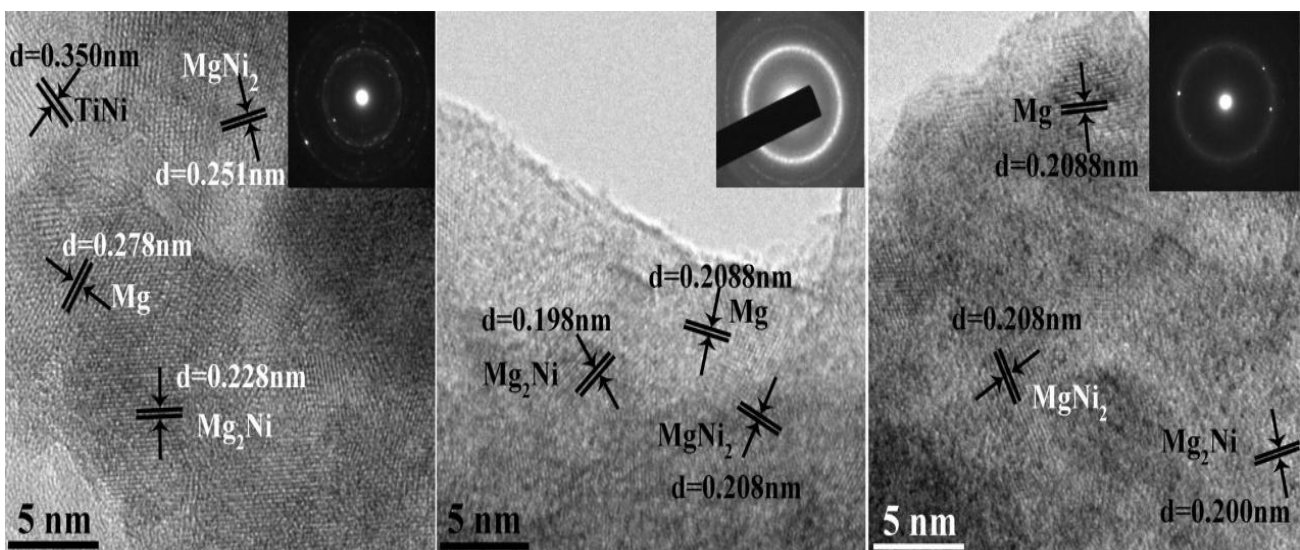


Fig. 2 HRTEM micrographs of ball-milled $Mg_xNi_{100-x}+5$ wt.% TiF_3 ($x=50, 60, 70$) hydrogen storage alloys

Electrochemical Discharge Capacity and Cycle Stability

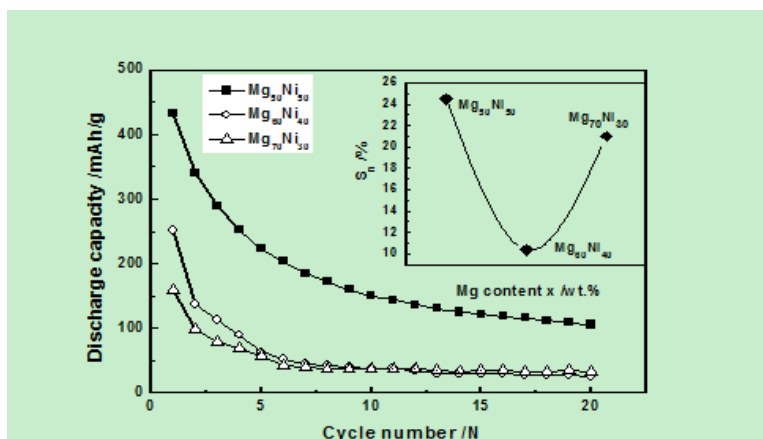


Fig. 3 Relationship between discharge capacity and cycle number for ball milling $Mg_xNi_{100-x}+5wt.\%TiF_3$ ($x=50, 60, 70$) composite hydrogen storage alloys

Fig. 3 shows the relationship curves between discharge capacity and cycle stability of ball-milled $Mg_xNi_{100-x}+5wt.\%TiF_3$ ($x=50, 60, 70$) composite hydride storage alloys. It is found that all milling alloy examples exhibit excellent activation ability, and obtain the maximum discharge capacity at the first charge and discharge cycle. It is well known to all that the activated ability of alloy electrode principally depends on the change of the internal energy of the hydride system before and after absorbing and desorbing hydrogen. That is to say that the smaller the internal energy is, the better the activated properties of alloy electrode will be. For superior activation capability the nanocrystalline/amorphous and multiphase structure formed in the process of mechanical milling is mainly responsible because lots of grain boundaries of the former probably act as buffer area which can release the lattice distorted and the strain energy accumulate during hydrogen absorption process and numerous phase boundaries of the latter provide effective paths for hydrogen atoms to diffuse. Besides, from Fig. 4 we can clearly find that the increase of Mg content gives rise to the decrease of the discharge capacity, namely the maximum discharge capacity is 431.7 mAh/g, 250.6 mAh/g, 160.1 mAh/g corresponding to the Mg content of $x=50, x=60, x=70$, indicates that the growing of Mg content determines to improving the discharge capacity of milled $Mg_xNi_{100-x}+5wt.\%TiF_3$ ($x=50, 60, 70$) composite hydrogen storage alloys. Some explanations can be provided as the reason why the rising of amount of Mg impairs the discharge capacity of experimental alloys. On the one hand, the $MgNi_2$ and Ni phase only act catalytic function and not hydrogen forming phase. On the other hand, strengthening the glass forming ability changes the proportion of amorphous and nanocrystalline, affecting the electrochemical discharge capacity of ball-milled alloy samples further.

Illustrated in Fig. 4 are the XRD profiles of ball milling $Mg_xNi_{100-x}+5wt.\%TiF_3$ ($x=50, 60, 70$) hydrogen storage alloys after absorbing hydrogen. It is evident that the increase of atomic Mg content makes the hydride of prepared alloy samples change significantly. The hydride composes of major phase Mg_2NiH and Mg_2NiH_4 for $x=50$ alloy. With respecting to $x=60$ and $x=70$ alloys, the Mg_2NiH_4 phase of hydride declines dramatically comparing with $x=50$ alloy. Meantime, the XRD patterns exhibit the emergence of lots of MgH_2 phase. It has come to light that the thermodynamic stability of Mg_2NiH_4 phase is smaller than that of MgH_2 phase, which may be the main reason to make the milled $Mg_{50}Ni_{50}+5wt.\%TiF_3$ alloy possess optimum electrochemical discharge capacity.

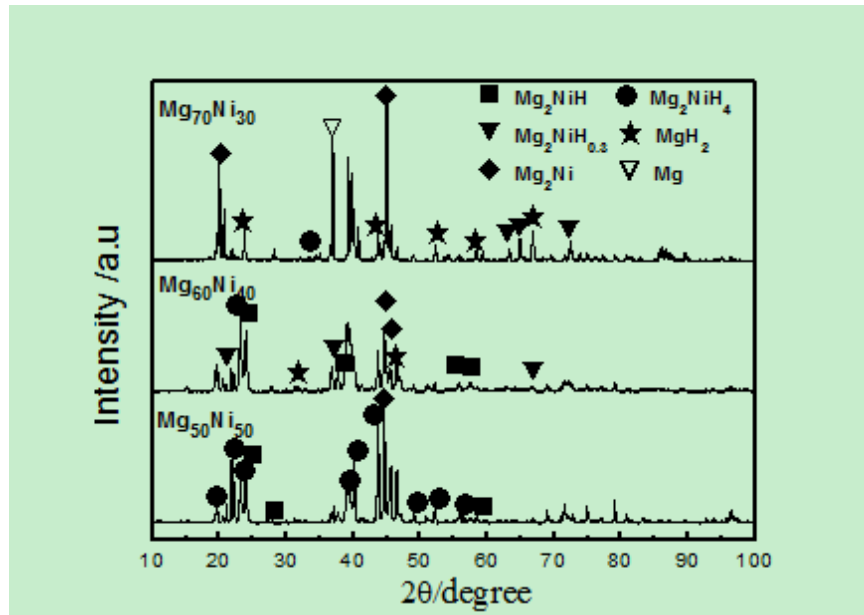


Fig. 4 XRD patterns of ball-milled $Mg_xNi_{100-x}+5$ wt.% TiF_3 ($x=50, 60, 70$) composite hydrogen storage alloys after absorbing hydrogen

The cycle stability, being an important property parameter, which used to evaluate whether an alloy electrode can be applied as negative electrode materials in Ni-MH battery is signified by the capacity retention rate (S_n), defined as $S_n = C_n / C_{max} \times 100\%$ where C_{max} and C_n are the maximum discharge capacity and the discharge capacity at the n th charge-discharge cycle respectively. The plot of evolution of the S_n values of ball milling alloy samples depending on Mg content is inserted in Fig. 3, showing that $Mg_{50}Ni_{50}+5wt.\%TiF_3$ exhibits the best electrochemical cycle stability. The above result can be ascribed to the adequate proportion of nanocrystalline and amorphous forming in experimental alloy. Especially, the emergency of the amorphous structure exerts not only enhances electro-catalysis but also corrosive resistance, which is benefit for ameliorating the electrochemical discharge and cycle stability performance, as reported in literature [9]. The other reason meliorating the cycle stability of alloy electrode is the presence of TiNi phase owing to such a fact that it is helpful for the improvement of cycle life of ball-milled alloy [10].

Conclusions

The Mg-Ni composite hydrogen storage alloys with nanocrystalline and amorphous were prepared through the addition of TiF_3 combining with mechanical ball-milled technology. The microstructure analyses indicates that the ball milling $Mg_xNi_{100-x}+5wt.\%TiF_3$ ($x=50, 60, 70$) alloys comprise multiphase and nanocrystalline/amorphous structure including Mg_2Ni , Ni, TiNi and $MgNi_2$ phase, the additive TiF_3 may be helpful for the formation of such structure. The ball milling $Mg_{50}Ni_{50}+5wt.\%TiF_3$ alloy exhibits the best electrochemical discharge capacity and cycle stability, to be attributed to the optimum proportion of nanocrystalline and amorphous in it. Moreover, the forming Mg_2NiH_4 phase of milling $Mg_{50}Ni_{50}+5wt.\%TiF_3$ alloy after absorbing hydrogen is other main factor resulting in the optimized discharge capacity of it.

Acknowledgements

This work is supported by National Natural Science Foundations of China (51161015 and 51371094), Natural Science Foundation of Inner Mongolia, China (2013MS0722), Innovation Foundation of Inner Mongolia University of Science and Technology (2014QDL015).

Reference

- [1] J. Jiang, M. Gasik, An electrochemical investigation of mechanical alloying of MgNi-based hydrogen storage alloys, *J. Power Sources*. 89 (2000) 117-124.
- [2] H. Simchi, A. Kafloub, A. Simchi, Synergetic effect of Ni and Nb₂O₅ on dehydrogenation properties of nanostructured MgH₂ synthesized by high-energy mechanical alloying, *Int. J. Hydrogen Energy*. 34 (2009) 7724-7730.
- [3] K. Iyajutti, Y. Kawazoe, M. Rajarajeswari, Aluminum hydride coated single-walled carbon nanotube as a hydrogen storage medium, *Int. J. Hydrogen Energy*. 34 (2009) 370-375.
- [4] W.H. Liu, H.Q. Wu, Y.Q. Lei, Effects of substitution of other elements for nickel in mechanically alloyed Mg₅₀Ni₅₀ amorphous alloys used for nickel—metal hydride batteries, *J. Alloys Comp.* 261 (1997) 289-294.
- [5] H.Y. Shao, K. Asano, H. Enoki, Preparation and hydrogen storage properties of nanostructured Mg–Ni BCC alloys, *J. Alloys Comp.* 477 (2009) 301-306.
- [6] Y. Feng, L.F Jiao, H.T. Yuan, Effects of amorphous CoB on the structural and electrochemical characteristics of MgNi alloy, *Int. J. Hydrogen Energy*. 32 (2007) 2836-2842.
- [7] R. Janot, A. Rougier, L. Aymard, Enhancement of hydrogen storage in MgNi by Pd-coating, *J. Alloys Comp.* 356-357 (2003) 438-441.
- [8] A. Gasiorowski, W. Iwasieczbo, D. Skoryna, H. Drulisb, M. Jurczyk, Hydriding properties of nanocrystalline Mg_{2-x}M_xNi alloys synthesized by mechanical alloying (M=Mn,Al), *J. Alloys and Comp.* 364 (2004) 283-288.
- [9] S. Deledda, A. Borissova, C. Poinignon, H-sorption in MgH₂ nanocomposites containing Fe or Ni with fluorine, *J. Alloys Compd.* 404-406 (2005) 409–412.
- [10] J. Charbonnier, P. de Rango, D. Fruchart, Hydrogenation of transition element additives (Ti, V) during ball milling of magnesium hydride, *J. Alloys Compd.* 383 (2004) 205–208.